Journal of Cultural Heritage 58 (2022) 274–283

Contents lists available at ScienceDirect

Journal of Cultural Heritage

journal homepage: www.elsevier.com/locate/culher

New methodological approaches in Reflectance Transformation Imaging applications for conservation documentation of cultural heritage metal objects

Amalia Siatou[a,b,*], Marvin Nurit[b], Yuly Castro[b], Gaëtan Le Goïc[b], Laura Brambilla[a], Christian Degrigny[a], Alamin Mansouri[b]

[a] Haute Ecole Arc Conservation-Restauration (HE-Arc CR), University of Applied Sciences and arts Western Switzerland (HES-SO), 2000, Neuchâtel, Switzerland

[b] Laboratory of Imaging and Artificial Vision (ImViA) - EA 7535- Université de Bourgogne Franche-Comté (UBFC), 21000, Dijon, France

ARTICLE INFO

Article history:
Received 8 March 2022
Accepted 17 October 2022
Available online 12 November 2022

Keywords:
Reflectance Transformation Imaging
Conservation documentation
Feature maps
Saliency maps
Distance measurements maps

ABSTRACT

Imaging techniques, along with their subsequent processing and analysis, are of utmost importance in the visual documentation of conservation processes of cultural heritage (CH) objects. Amongst them, Reflectance Transformation Imaging (RTI) is being used as a tool for the enhancement of surface topography, such as decorative details. This paper proposes a new approach based on advanced RTI data processing and analysis to document the condition of metal artefacts or monitor their conservation treatments. First, the methodology for mapping geometric and statistical information from the stack of RTI image data and their relation to the surface topography and the appearance attributes resulting in feature maps is described. Additionally, the possibility of quantifying intra- or inter-surface changes based on saliency and distance measurements by applying the Mahalanobis distance (MD) on feature maps is demonstrated. This methodology is then used for documenting the condition and monitoring the cleaning treatment of a late Roman coin.

Introduction

Conservation documentation can be defined as the textual and visual records collected during the care and treatment of an object [1]. Visual records are a crucial component, corresponding to recording an object's visual appearance and surface topography at a given time (i.e., condition assessment) or after an action (e.g., conservation treatments).

The visual appearance of an object is perceived through its interaction with light. To characterise appearance, different attributes, which are directly linked to the physical and optical properties of the surface, are used. Four essential attributes are interrelated and, when measured, can result in the "total visual appearance" of an object. These attributes are colour, gloss, translucency and texture [2,3]. For cultural heritage (CH) metal objects, three attributes are of higher importance: colour, gloss, and texture. Colour can be used to identify the metal's composition and equally its corrosion products that create characteristic colours for each metal. Gloss and texture, which are usually interrelated, can either describe the manufacturing process, decoration or surface finish but can also signify corrosion or wear. These attributes can reveal technological characteristics, describe the object's condition, or help monitor conservation treatments in conservation documentation.

The surface topography of an object is directly related to the micro-geometry of the surface. It represents the deviation of the heights from a plane and is therefore interrelated with the surface texture. In computer vision, accurate documentation can be obtained through the photometric stereo, where the surface is computed based on its reflectance. This method calculates the surface orientation according to pixel-level light intensity [4]. The local surface orientation and its subsequent illumination direction depend on the surface properties, and thus the geometry can be calculated based on the directionality of the surface normals.

Abbreviations: CH, Cultural Heritage; DMM, Distance Measurement Map; LPs, Light Positions; MD, Mahalanobis Distance; RTI, Reflectance Transformation Imaging.

* Corresponding author.
E-mail address: amalia.siatou@he-arc.ch (A. Siatou).

https://doi.org/10.1016/j.culher.2022.10.011

In conservation documentation, different imaging techniques are used to characterise the appearance and the topography of a surface. This paper examines the application of Reflectance Transformation Imaging (RTI). RTI has been mainly utilised to study technological and decorative features of surfaces, such as enhancing the legibility of epigraphs or surface details [5–9]. However, there is a growing interest in exploiting RTI data to document or monitor conservation processes. Most references present case-study orientated approaches [6,7,10–14].

Nevertheless, different methods are proposed for visualisation and data analysis. An extensive state of the art in RTI was presented by Pintus et al. (2019) [15].

This paper focusses mainly on methodologies for surface characterisation and change detection related to data processing of raw RTI image stacks without integrating fitting models in the surface analysis. Towards this, few authors are have presented relevant work. Manfredi et al. (2013, 2014) proposed a methodology that examines the documentation of topographic changes using the surface normals for characterising the directionality of change on a mock-up painting before and after damage [16,17]. Dulecha et al. (2019) propose a MLIC (multi-light image collections) approach for edge detection and Convolutional Neural Networks protocol for supervised classification with the goal to automatically detect cracks on paintings [18]. Finally, Corregidor et al. (2020) extended edge detection analysis to RTI data for documenting damaged areas on coins [19].

Research aim

This research proposes a new data processing methodology for exploiting RTI data to provide accurate tools for conservation documentation based on studying the appearance attributes and the geometry of CH metal objects. The goal is to use RTI data to document changes on metal surfaces using three different types of maps resulting from the proposed methodologies, namely feature maps, saliency maps, and distance measurement maps.

These maps can be of interest in condition assessment and monitoring/documenting conservation treatments since they can provide accurate and automated documentation processes for the visual assessment of surfaces and change tracking. More particularly, the influence of the visual appearance due to corrosion and cleaning is demonstrated.

Theoretical aspects and methodology

Reflectance transformation imaging

RTI is a Multi-light image collection (MLIC) technique that involves varying the light directions in a hemispherical light array around a surface, to provide multi-angle photographic documentation. The general principle is well described in the literature [20–22]. In outline, the surface under examination is placed opposite a camera. A series of images are acquired from different illumination angles while the camera and the surface remain fixed (Fig. 1a and 1b). This results in an exploitable RTI image stack, also called photometric stereo images, from different light positions that can be used for further data processing and analysis (Fig.1c).

There are different methods for acquiring these types of data, ranging from freeform acquisitions to domes [7,20,21] or, in more recent cases, robotic arms [23]. In terms of data processing and interpretation, the most common approach is through relighting, surface enhancement or studying the surface normals with different existing visualisation tools. These tools use fitting algorithms that combine the raw image data. There are different proposed methods and algorithms to achieve this [21,24–26], but their analysis is outside the scope of this paper.

This paper proposes a new data processing approach that could lead to a more accurate characterisation of the examined surfaces based on features.

Feature maps

In computer vision, the term "feature" refers to locations (corners, borders, centres, etc.) of an image that can characterise it. In this context, feature extraction/detection is a type of information reduction. These locations can be described through descriptors (vector of features). For RTI data, the features are not limited to a few locations but are calculated at every pixel and are reduced to a single image/map. Therefore, a feature results from an algorithmic or mathematical function applied to every pixel of the RTI stack giving rise to a feature map. In more detail, for an RTI acquisition of N images (Fig. 2), each pixel of the surface is associated with an N size vector that corresponds to the local angular luminance $L(i,j,k)$. Then, depending on the selected feature, the corresponding algorithm is applied to the N images for each pixel position $L(i,j,k)$, where i and j are the pixel's coordinates and k the image number of the stack. This results in a map (grey or false colour) that incorporates the features corresponding to the per-pixel result of the mathematical function applied at each position $L(i,j,k)$.

The available features can be estimated per pixel from the RTI image stack and are then combined into a single visualization (feature map). Features are divided into two main categories based on their functionality, namely geometric and statistical, and are listed in Table 1. Geometric features are related to the surface's directional, curvature or angular characteristics. They are linked to surface topography and thus can give information associated with manufacturing techniques, decorative characteristics

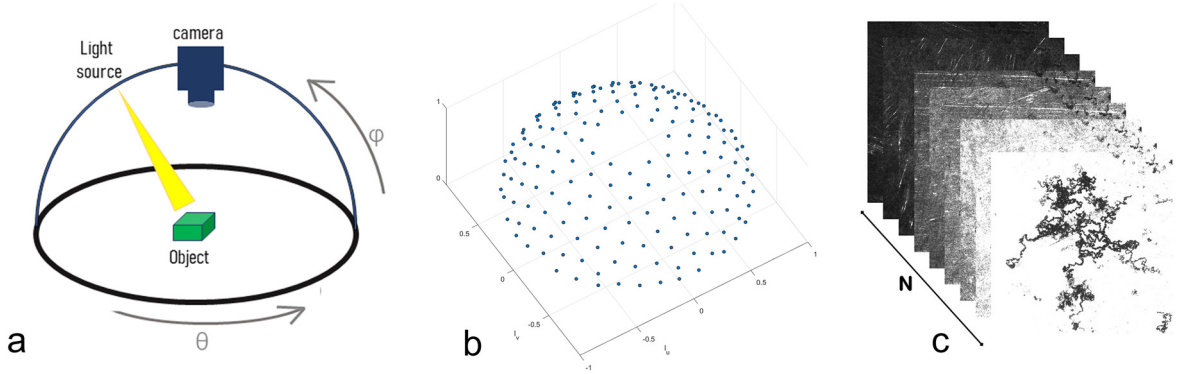

Fig. 1. Schematic Representation of RTI methodology a. Dome based RTI set-up b. Homogeneous distribution of the light positions creating a hemisphere c. Stack of raw RTI images illuminated at different light positions.

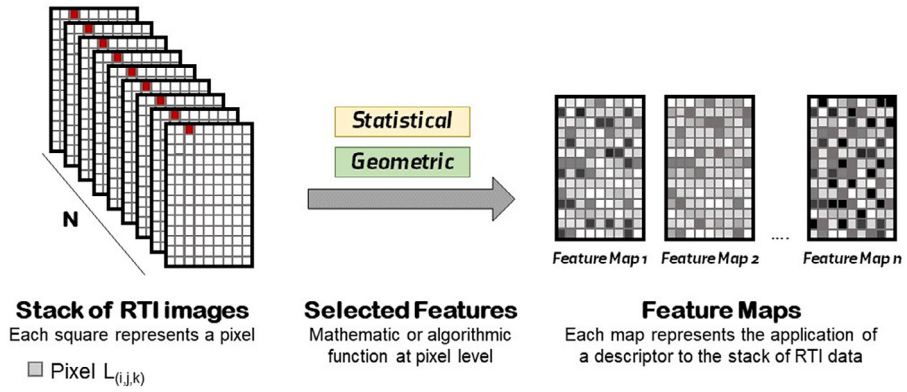

Fig. 2. Schematic representation of features maps methodology.

Table 1
Geometric and statistical features that can be used for the feature maps [Nurit 2022].

List of possible features [27]			
Geometric		Statistical	
Normal	A vector perpendicular to a surface for each pixel in the cartesian space.	Mean, energy	The average value of the per-pixel reflectance and the sum of its squared value respectively.
Dz*, Dx, Dy	The directional slopes of each axis of the normal.	Median	The middle point of the per-pixel dataset.
Kxx, Kxy, Kyy	The curvature as a derivative of Dx or Dy to the respective axis.	Standard Deviation	The dispersion of the pixel values.
Dip Angle*	The orientation of φ to the plane.	Coefficient of Variation	The ratio of the standard deviation to the mean.
Azimuth Angle	The orientation of the local texture.	Kurtosis	The distribution of the pixels reflectance by comparing the weight of the distributions tail to the centre.
Kmax, Kmin	The maximum and minimum of the normal curvature respectively (principal curvatures).	Skewness	The distribution based on its deviation from a normal distribution.
Kmean*, Kgaussian*	The average and the product of the principal curvatures respectively.	Entropy	Quantitative measure of the randomness of the pixels for the light positions.
Shape Index*	Description of the form of the curvature.	Max, Min	Maximum and minimum values respectively.
Curvedness*	The measure of the intensity of the curvature of a point.	Dynamic Ratio	The ratio between the maximum and the minimum.

* Invariant to surface rotation.

(e.g. tool marks) or surface defects (e.g. cracks) and of documentation processes (e.g. development of oxides) that provoke changes to the surface topography. Statistical features result from calculations applied, per pixel, to the stack of RTI data, providing information related to the reflectance response of the surface for the different light positions. These features are highly affected by the appearance attributes of the surface since colour, gloss, and texture can cause differences when light is reflected from a surface. Statistical features can separate information based on the changes in the specularity of the surface or the absorption of light. Therefore, information related to colour, gloss or texture change (e.g. corrosion products versus metal substrate) can be accurately depicted.

An application example of features maps is presented in Fig. 3. A region of interest (ROI) of an iron object exhibiting visible signs of corrosion was selected. Its surface shows signs of wear (scratches) as well as two different types of localised corrosion: the most visible in the form of a filament (filiform corrosion) and a reddish layer extending around the filament. Fig. 3b is a photograph of the ROI. Fig. 3a presents a statistical map based on the calculation of the "mean", namely the arithmetic mean (μ) of the reflectance of each pixel *(L(i,j))* at each different light illumination position (*k*, Fig. 2). The result is a map where each pixel represents the average value of the reflectance response. This map helps accurately depict the corroded areas since they differ in colour and texture from the metal substrate, giving a different reflectance response. The filament (high texture and dark colour) reflects less light and therefore has a lower mean value in contrast to the substrate. In this case, the reddish corrosion around the filament shows higher mean reflectance than the metal and can be detected.

Fig. 3c presents a geometric map based on the dip angle estimation. This map depicts the surface topography changes in terms of angular differentiation. Areas parallel to the camera correspond to zero values (darker areas), whereas areas with higher topography, like the localised corrosion (filament), correspond to higher angular differences (lighter areas). Equally, surface defects like scratches are also depicted since their orientation differs from the surface. On the contrary, this map does not detect the reddish layer, which creates low topographic changes.

Mahalanobis distance for surface comparison

As a further step of processing RTI data, the features can be combined in descriptors, which are examined in a multivariate space using the Mahalanobis Distance (MD). MD can measure either the similarity or dissimilarity between multivariate data. It is the distance between a multidimensional point described by a

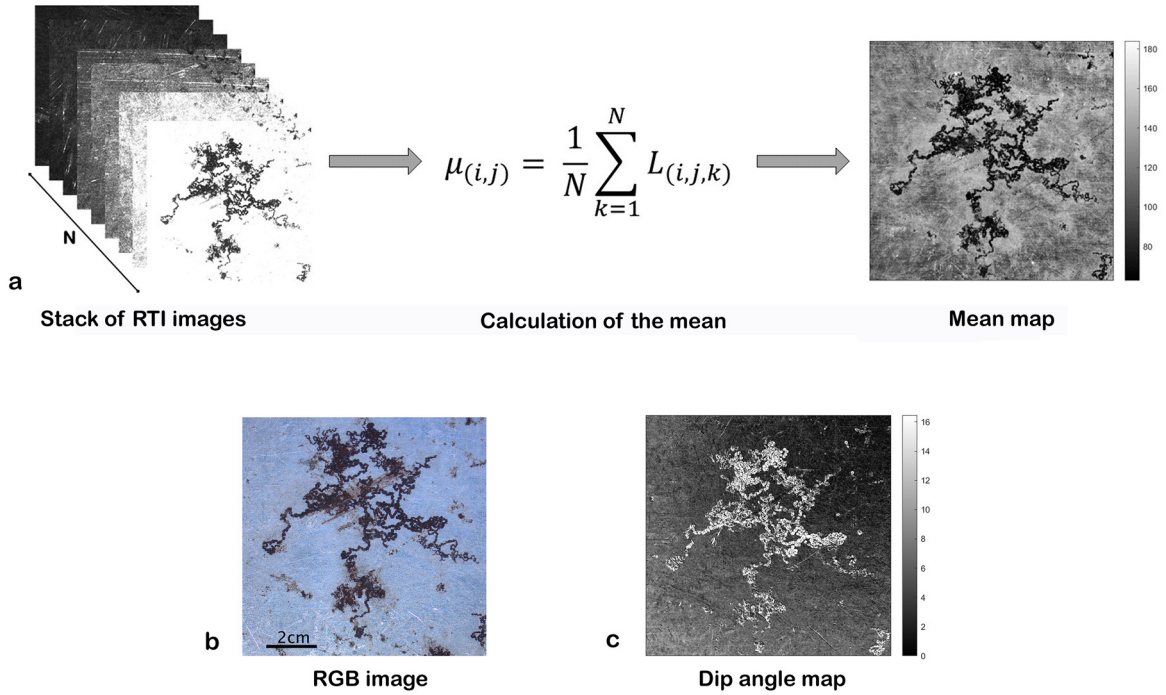

Fig. 3. Example of selected feature maps for the corrosion study of a metal surface a. Schematic representation of the calculation of the "mean map" b. Photograph of the ROI c. Dip angle map.

multivariate vector and a distribution of points (also multivariate) [28,29]:

$$MD_{(x)} = \sqrt{(x-\mu_y)\Sigma^{-1}(x-\mu_y)'}$$

where

x = data corresponding to multivariate vector of the point with different variables,
y = reference corresponding to the distribution of points for the same variables,
μ_y = mean value of y,
Σ = covariance matrix of independent variables.

MD has in the past been used for change detection in imaging with interest in spatial and temporal changes of earth's surface. First Osmar (2011) for calculating the magnitude component of the spectral direction of change in Change-Vector Analysis [30]. Wang (2020) used MD for metric learning methods by calculating similarities and dissimilarities to propose a new approach for creating different images for SARs [31].

For RTI data, x corresponds to an $n-by-j$ numeric matrix where n is the number of pixels of a selected feature map and j is a selection of variables (features values). On the contrary, y corresponds to a $p-by-j$ numeric matrix. In both cases, p is the total number of pixels of the selected feature map and j the selected variables. The MD calculates the distance of the pixel x from the mean of y, resulting in an $n-by-1$ vector.

In this paper, the MD is examined in two ways for measuring the distances of correlated variables that can reveal areas of low or high similarity, visualised through distance measurement maps (DMM). For this application, x is consistent with the surface's pixels, whereas y corresponds to all the selected pixels to be compared to, called from now on the "reference surface". The variables are equivalent to descriptors. In the first case, MD is applied to the same surface (intra-surface) and in the second case (inter-surface), between different surfaces or between different ROIs of the same surface. In both cases, each pixel descriptor is compared to a global neighbourhood (the entire surface or selected areas) using the MD, creating thus a DMM. A schematic representation of the application of MD on RTI data is given in Fig. 4.

The resulting maps (Saliency or Distance Measurement) can contain different types of information. Any combination of the above descriptors is possible. A logical grouping of the features is used herein and, more specifically, the "geometric features" that encompass all features related to directionality, curvature and surface topography and the "statistical features" that refer to all features related to descriptive statistics (Table 1).

Intra-surface comparison

Intra-surface comparison is the DMM resulting from the application of the MD on the same surface. Using the calculated features, each pixel of the examined surface can be compared to a global neighbourhood of the reference surface and measure how it stands out from the total; this is called saliency. In this case, both the examined and the reference surfaces are the same resulting in saliency maps. These maps allow for surface analysis based on descriptors for identifying distinctive features of the surfaces themselves.

Fig. 5a explains the creation of these maps schematically. First, starting from the stack of RTI images, the most relevant features are selected, which results in feature maps. Then, a descriptor (combined features) of a pixel is correlated using MD with the descriptors of all the pixels. The resulting saliency map depicts surface pixels that differ significantly from the mean value of the selected variables (higher saliency).

Saliency maps can help further characterise a surface by documenting the variability based on selected features applied to an RTI dataset. Therefore, the appearance attributes or localised surface geometries that greatly differ from the average values of the surface become prominent.

The same application example (Fig. 3) used for the feature maps was examined in terms of saliency (Fig. 5b). A series of statistical features were selected as variables for studying the surface saliency. Then, the saliency map was created incorporating this

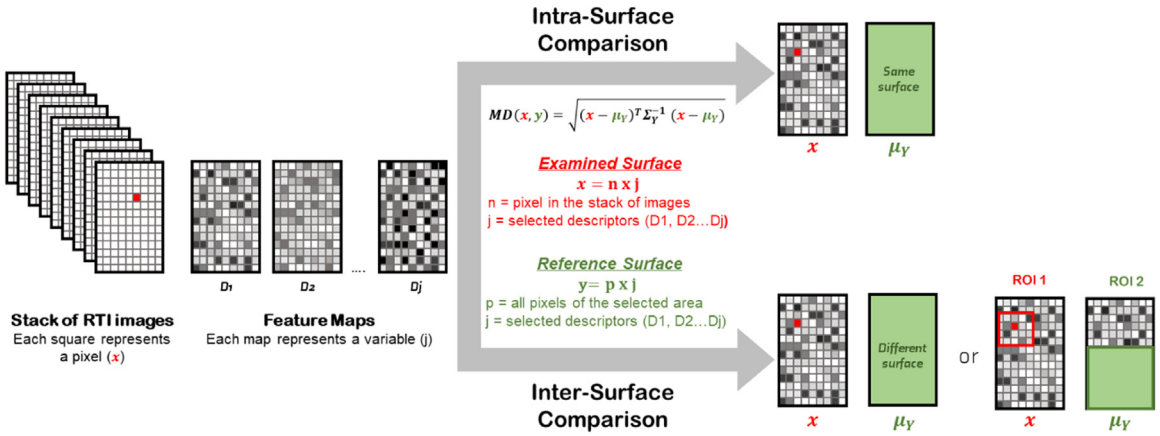

Fig. 4. Schematic representation of RTI data analysis for the calculation of Mahalanobis Distance.

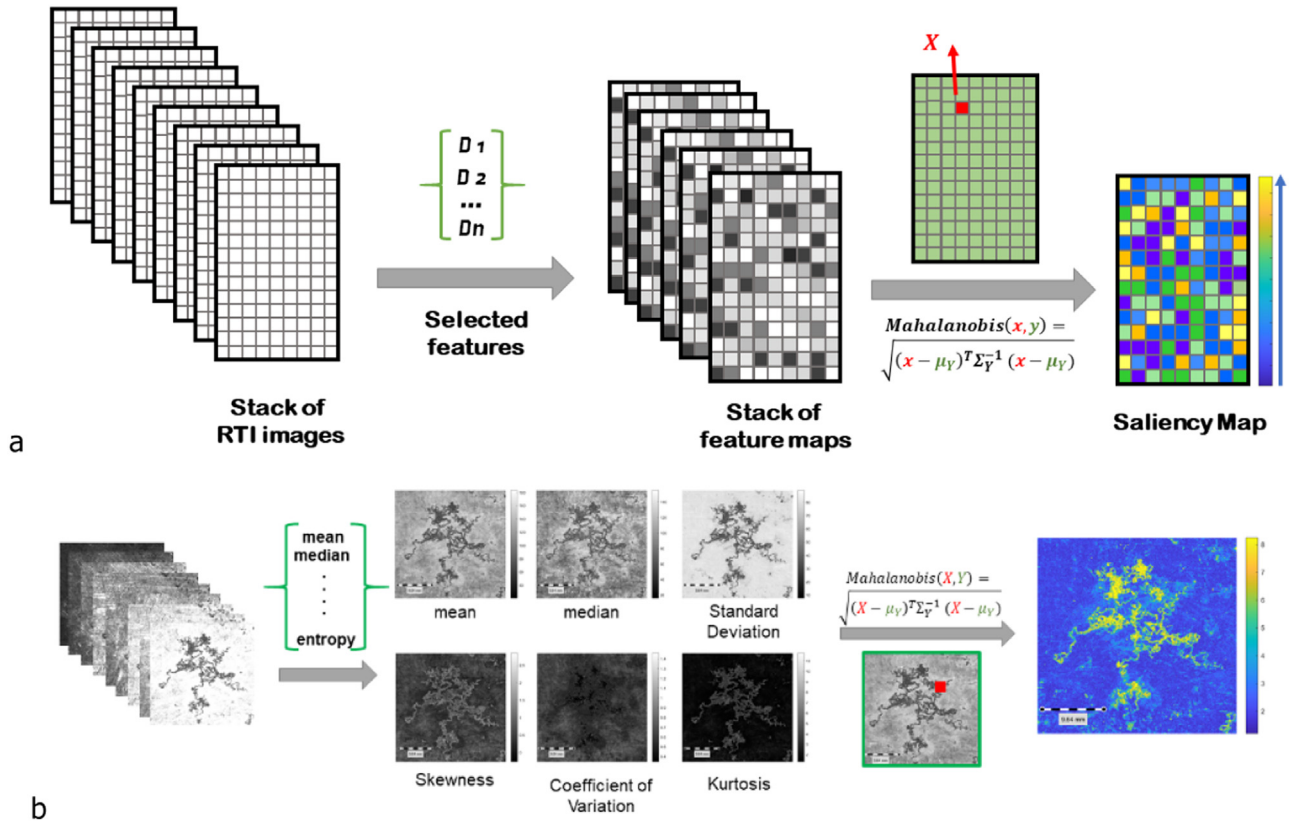

Fig. 5. a. Schematic representation of saliency maps methodology b. Example of saliency maps for the corrosion study of a metal surface.

statistical information. The statistical feature map provided data demonstrating that the filament is darker in colour and has a less specular reflectance than the underlying metal. This is consequently depicted in the saliency map, where it is evident that the area with the filament differs greatly in comparison to its metal substrate. This differentiation is caused mainly by the differences in the physical properties between the filament (highly textured surface, darker colour) and the metal substrate (high specularity, lighter colour) that create a high variance in the pixel reflectance response.

Inter-surface comparison

Inter-surface comparison is the DMM resulting from the application of the MD between two surfaces or two ROIs of the same surface. To achieve this, a set of features is selected following the methodology described above. Then the distance measurement is calculated for each feature by computing the MD between the examined and the reference surface. The examined surface equals the surface that provides the pixels (points), and the reference surface is the neighbourhood of pixels to which they are compared. Each pixel of the examined surface is thus calculated against the mean value of the reference surface's same variable (feature). Fig. 6a explains the creation of these maps schematically. Relevantly to the saliency maps, the MD values of all the examined descriptors create a unique map depicting the differences between the compared surfaces. These maps can help identify differences between surfaces (e.g. monitor changes during conservation treatments or evolution of corrosion) or help characterise or isolate the optical and physical properties of the surface when applied to different ROIs of the same surface.

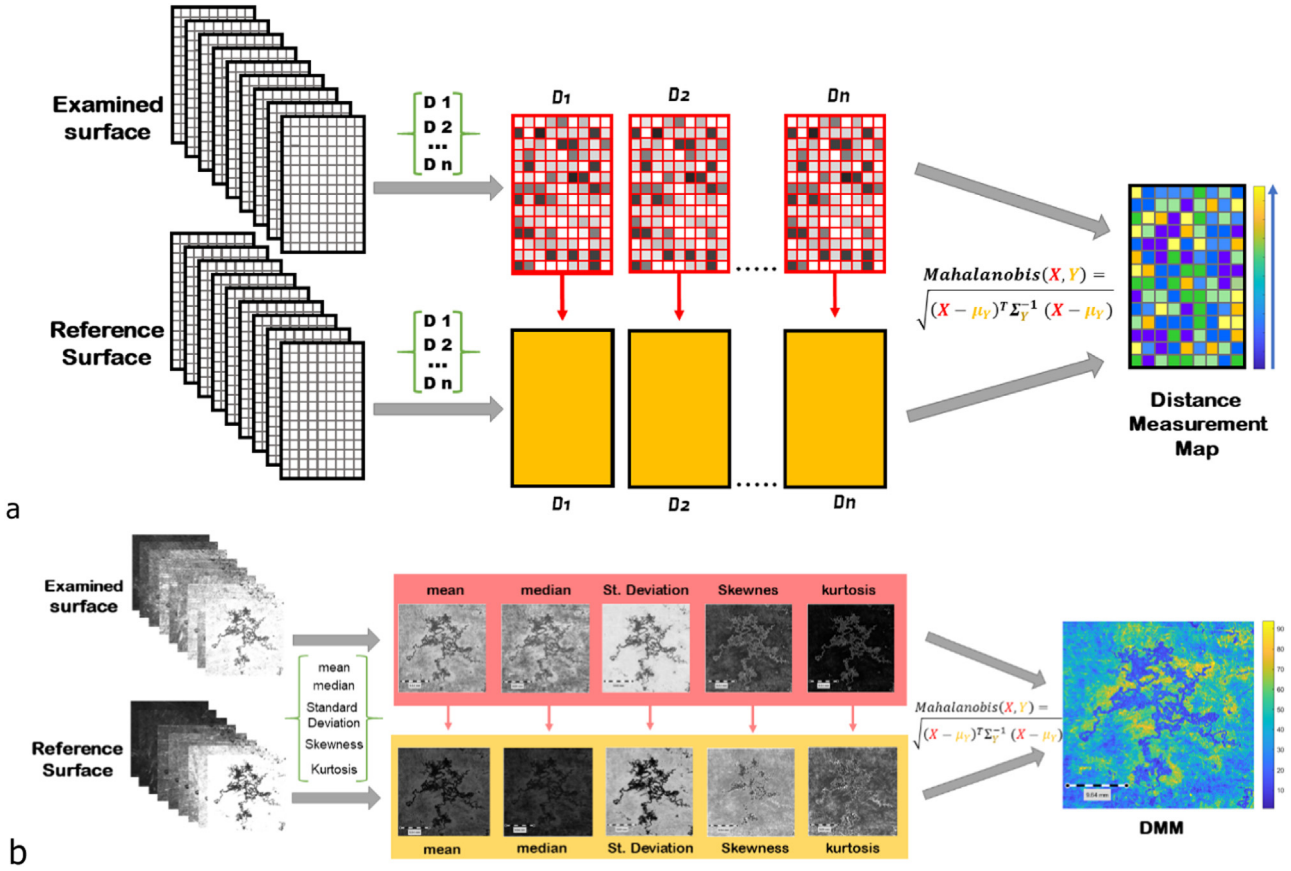

Fig. 6. a. Schematic Representation of distance maps methodology b. Example of distance maps for the corrosion study of a metal surface.

An example of the methodology is presented in Fig. 6b. The same surface (Fig. 3) was examined under different light exposure times. The exposure time was set at 400 ms and 150 ms for the reference and the examined surface, respectively. Even though the stack of the acquired images is seemingly similar, the effect of the lighting difference is depicted in the DMM. This example demonstrates the influence of the selection of light exposure conditions for studying specular surfaces. The filament, having low reflectivity and high absorption properties, is not highly affected by the difference in light exposure conditions. Similarly, the high reflective areas are minimally affected by the changes in the light intensity. However, areas with higher differences (yellow areas) surround the filament are depicted in the inter-surface map. These areas correspond to the reddish corrosion around the filament that has different optical and physical properties (thin uniform layer), which causes differences in the reflectance response of the surface and is affected by the exposure time.

Application in conservation documentation

The feasibility of applying this methodology for conservation documentation is demonstrated through the condition assessment and monitoring of cleaning treatment of a late-Roman coin from a burial environment. RTI data were collected before, during and after cleaning, and the resulting maps were studied.

RTI setup and data acquisition

For this study, a dome with motorised functions equipped with a single light source (cold white LED, 6500 K) was used. An industrial, monochromatic camera (CMOS sensor: Sony IMX304, resolution, 4112 (H) x 3008 (V)) was placed at the top of the dome, and a machine vision lens was attached to the camera. A user interface allows the control and setting of the experimental parameters. This set-up provides controllable functions in reproducibility and repeatability of acquisitions, making surface comparison possible.

To ensure reproducibility, the acquisition conditions were kept constant for each conservation documentation step (before/ during/ after cleaning). More specifically, the coin was placed manually in the dome's centre. Then, the acquisition of 150 images corresponding to 150 light positions (LPs), homogeneously distributed, covering a hemisphere around the coin was applied. The exposure time was estimated for "before cleaning" and was kept at 500 ms.

The resulting stack of images require the following preprocessing steps:

1. Illumination correction by applying a flat field correction: The light source is not collimated, resulting in a non-uniform surface illumination. Flat field correction was applied to eliminate the inhomogeneity of the light distribution. A per-pixel coefficient was applied to the raw image data based on the mean pixel value of the central location. A white wavelength calibration standards (Spectralon® 99%) was used to calculate this coefficient. An acquisition similar to that of the coin (same magnification, same LPs) was obtained, and after applying a low pass filter, the mean pixel value of the central area (800 × 800 pixel window) was estimated per light position. This value was then used to calculate a pixel-wise correction coefficient matrix for each LP. This coefficient matrix was then applied to the coin's raw image stack, resulting in homogeneous lighting for each illumination angle. The corrected images were used for the implementation of the methodology mentioned above.

2. Image registration: The placement in the centre of the dome was performed manually; therefore, post-processing image registration, using multimodal translation, was applied to each separate image stack to allow for better visual comparability of results and selection of the ROI. However, it must be noted that the application of MD corresponds to the comparison between each pixel and the distribution of pixels; therefore, image registration is not necessary for the calculation, except in the case of the features that are not invariant to rotation (Table 1).
3. ROI selection: The map calculation is performed on the entire imaged surface. In the case of the coins having a round shape, the background can influence the results. To isolate the image's background, a mask was applied that allows the selection of the appropriate ROI.

The case study

The studied artefact is a late-Roman bronze coin of emperor Valens, struck at the mint of Nicomedia, 364–367 A.D. [32]. The chemical composition of the coin and the soiling elements were identified by X-Ray spectroscopy (Niton^{TM} XL3t XRF Handheld analyser, Thermo Scientific, 50 kV, Ag anode). The metal composition is a high copper (Cu) alloy with lead (Pb) and tin (Sn). In addition, the coin is covered with soiling elements consisting mainly of silicon (Si) and aluminium (Al), usually corresponding to silicon oxide (SiO_2) and aluminium oxide (Al_2O_3), commonly found in soils.

In its initial condition (before cleaning Fig. 7), most parts of the coin were covered by thick soiling encrustations, whereas the patina is visible in some areas with higher reliefs. Cleaning was performed by mechanical means following standard conservation-restoration practices. After cleaning, the coin presents a homogeneous dark patina for the most part; however, there are some minor areas where reddish corrosion products are visible as well as residual soiling. The different surface conditions (i.e. before/after cleaning) and materials (i.e. soiling encrustations, various metal corrosion products) correspond to distinctive appearance attribute characterised by differences in colour, texture and gloss. The soiling areas are lighter in colour and exhibit a rougher diffusive texture compared to the patina, which is darker in colour and presents a homogenous smoother texture. On the other hand, the reddish corrosion products are of a different colour and present higher specularity than the other materials.

Results

Feature maps

Feature maps present a great variety (Table 1); here, a selection of geometric and statistical features that better describe the surface topography and the appearance attributes, as well as their consequent change due to cleaning, are shown (Fig. 7). A full list of the resulting feature maps is presented in the appendix.

In terms of geometric features (Fig. 7), the normal maps demonstrate the overall change of the surface in terms of topography. The reliefs of the coin are covered with the soiling encrustations that, when removed, become more pronounced. Moreover, Dx, Dy and Dz maps can isolate the directionality of change, enhance the surface geometry and reveal the result of mechanical cleaning. More importantly, the Dz map demonstrates the areas with higher reliefs (dark areas) and, in the case of cleaning, can enhance the coin's legibility. The dip angle map provides more details on the changes in the surface texture since it describes the angular orientation of each pixel. Therefore, it detects better the changes in surface texture before and after cleaning and can be used for documenting cleaning processes with significant changes in textures, such as archaeological coins.

Regarding the statistical features (Fig. 7), the mean map depicts the average pixel values representing the reflectivity and colour of the surface. Before cleaning, the whitish and diffuse soiling encrustations present higher values than the patina. On the contrary, after cleaning, the lighter coloured areas become dark, corresponding to the darker colour of the surface (patina). In parallel, the higher reflectivity of the reddish corrosion products is also depicted by high pixel values. Equally, each statistical feature can provide additional information on the surface reflectance response and their comparison before and after cleaning clearly depicts the difference in the appearance provoked by the treatment. A common result of studying all statistical maps is that they demonstrate the homogeneity of the surface appearance after cleaning.

Saliency maps

Representative sets of features were selected to analyse the prominent attributes of the coin's surface, before and after cleaning, based on the results of the features maps. Since the surface changes relate to changes in the topography, the entire set of geometric features was studied (geometric features). However, the saliency maps related to geometry provide more information when the directional descriptors are separated. For example, the saliency map of "Dx, Dy, Dz", before and after cleaning, shows the areas where the surface details become more evident after removing the soiling elements. At the same time, the saliency maps of the statistical descriptors (statistical features, mean) mainly identify the areas where there is a higher difference in the reflectance response of the surface corresponding to the patina before cleaning and the reddish corrosion products after cleaning.

Distance maps

Distance measurements were performed before, during and after cleaning. The most important information was revealed when the coin was half cleaned (Fig. 8). A comparison between an unclean area (red circle Fig. 8) was used as a reference, and the MD in different sets of features was calculated for the entire surface (yellow circle, Fig. 8).

The geometric maps demonstrate the changes in the directionality of the reflectance of the surface in different areas. For example, in the left part (cleaned area), the borders of reliefs of the design show higher differences (yellow colours) and the decorative details are pronounced. Additionally, in the statistical maps, the cleaned area presents high differences from the uncleaned due to the surface colour and texture changes that result in more reflective surfaces.

Discussion

The appearance attributes of a surface like colour, texture, gloss and translucency are the main characteristics that change when a conservation treatment is performed. For example, cleaning will usually result in the change of colour and texture of the material; or, removing varnish from a painting will create a difference in the surface glossiness; these changes can be easily tracked with imaging techniques.

In this research, the surface characterisation is based on RTI data processing and can be obtained by examining the appropriate features that provide information on the visual appearance and surface topography. Therefore, an automated way of documenting the surface on any object that exhibits differences in the texture, colour or gloss and their resulting change through conservation-restoration treatments is feasible.

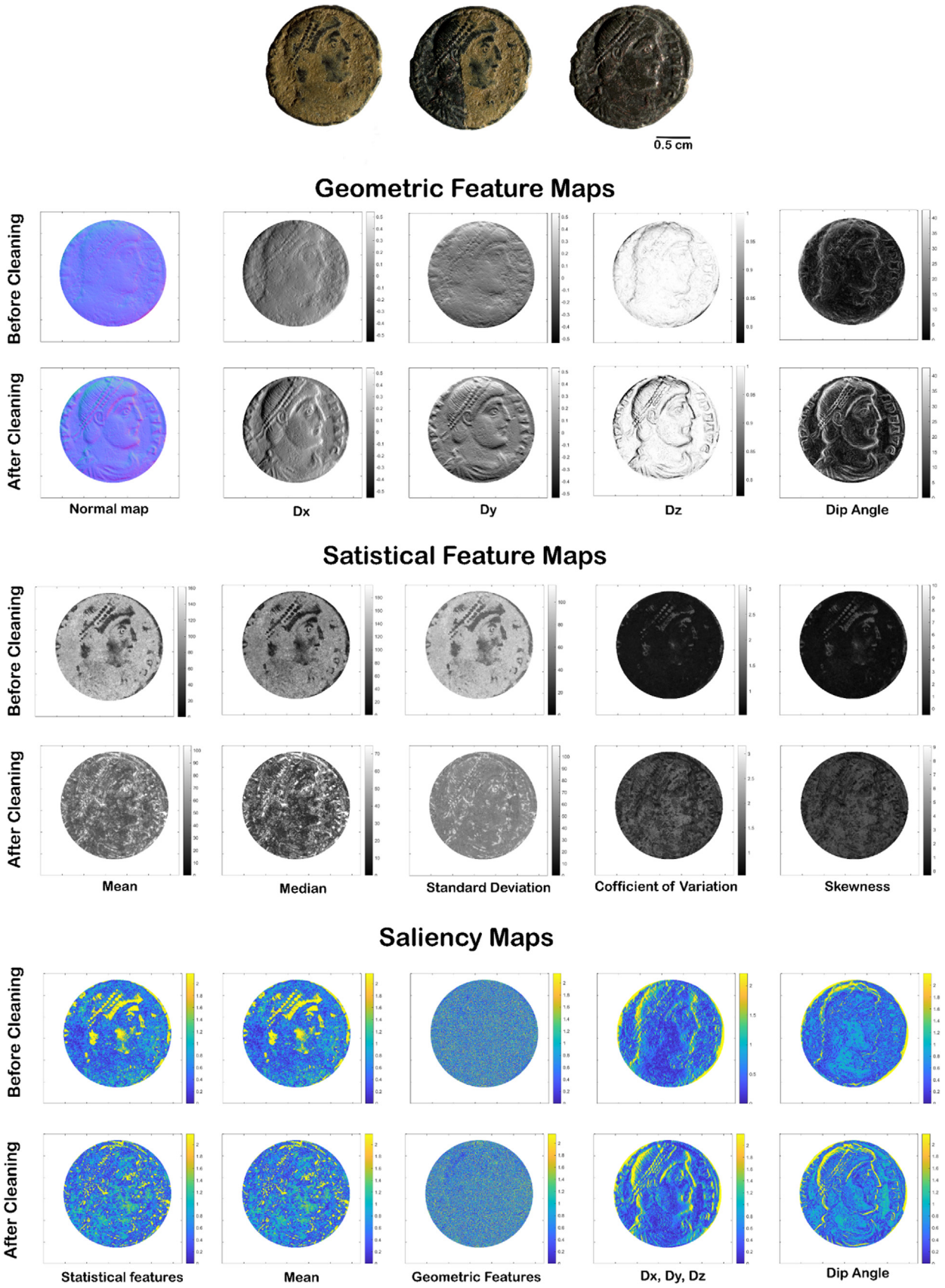

Fig. 7. Imaging performed on the coin Top: RBG images (before, during and after cleaning) Middle: Geometric and Statistical Feature Maps (before and after cleaning) Bottom: Saliency Maps (before and after cleaning).

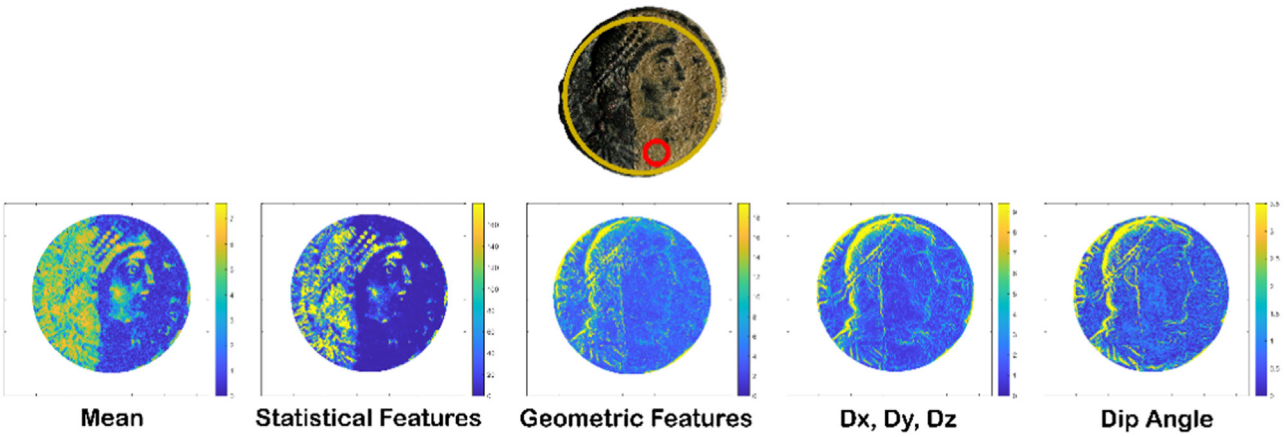

Fig. 8. Distance maps of the coin during cleaning. Top: red circle is the reference area (before cleaning) and yellow the examined one (the entire coin). Bottom: Selection of DMs that demonstrate the changes on the surface between the un-cleaned and cleaned area.

More specifically, geometric features are related to the directional, curvature and angular information of the surface as depicted from the light illumination in different directions. Statistical features are more linked to the appearance attributes of the surface since they provide information related to the reflectance response that is highly influenced by the colour, gloss and texture. This information is well defined in the features maps that can be used to accurately characterise an object's overall surface properties. Information related to technological characteristics, corrosion products and different manufacturing materials can be well documented in an automated way. Comparing the same maps between different conservation treatments or cross-time can provide information on the changes in surface properties.

Saliency and distance maps are adjustable and can provide multivariate information as well as a visualised quantification of change by comparison. In addition, these maps provide localised information based on global changes and, therefore, can estimate the degree of change. However, when studying changes at different time intervals or actions (i.e. before/after cleaning), the geometric reference points are calculated for each surface. Therefore, an arithmetic value of the degree of change at each interval cannot be estimated.

Even though the application of the methodology is straightforward, the selection of the appropriate maps and their interpretation require expertise in material properties and their consequent change when conservation treatments are applied, as well as knowledge in RTI imaging. The proposed methodology is more adaptable to cases with prominent topography and changes with well-defined appearance attributes. With the main interest of documenting high specular surfaces such as metals, the proposed methodology can be applied to different materials and surfaces to provide valuable information on the surface characteristics.

Conclusions

This paper proposes a new methodology for processing RTI data that can be used for automating conservation documentation processes, such as condition mapping. It demonstrates how the surface geometric characteristics and appearance attributes can be exploited for accurate and automated surface mapping. When the appropriate features are selected, information related to surface changes can be revealed. The topography of a surface and consequent geometry changes due to conservation treatments can be documented through geometrical maps. Statistical maps better document the surface changes in colour, texture and gloss. Saliency maps can reveal information on the different characteristics of the surface and help identify areas with prominent characteristics through classification. Distance measurements can track changes between surfaces or areas of the same surface and detect areas with high differences providing information on the extent and location of the change.

Funding

This research is funded by the European Union's Horizon 2020 research and innovation program Marie Skłodowska-Curie, under the "CHANGE" project (Cultural Heritage Analysis for New Generations), with grant agreement 813789. It was additionally supported by the French National Research Agency (ANR) through the projects NAPS (17-CE10–0005) & SUMUM (17-CE38–0004).

Acknowledgments

The authors would like to thank the numismatist Dr Eirini Marathaki for her precious help in identifying the coin's dating and provenance.

Supplementary materials

Supplementary material associated with this article can be found, in the online version, at doi:10.1016/j.culher.2022.10.011.

References

[1] M. Moore, Conservation documentation and the implications of digitisation, J. Conserv. Museum Stud. 7 (0) (2001), doi:10.5334/jcms.7012.
[2] C. Eugène, Measurement of 'total visual appearance': a cie challenge of soft metrology, in: Proc. 12th IMEKO TC1 Educ. Train. Meas. Instrum. TC7 Meas. Sci. Jt. Symp. "Man, Sci. Meas. 2008, 2008, pp. 61–65.
[3] CIE 175:2006, A Framework for the Measurement of Visual Appearance, ISBN 978 3 901906 52 7 (Ed.), Commission Internationale de l'eclairage (CIE), 2006.
[4] R.J. Woodham, Determining photometric stereo: a reflectance map, Image Underst. Syst. Ind. Appl. I (1978) 136–143.
[5] G. Palma, M. Corsini, P. Cignon, R. Scopigno, M. Mudge, Dynamic shading enhancement for reflectance transformation imaging, J. Comput. Cult. Herit. 3 (2) (2010), doi:10.1145/1841317.1841321.
[6] G. Earl, K. Martinez, T. Malzbender, Archaeological applications of polynomial texture mapping: analysis, conservation and representation, J. Archaeol. Sci. 37 (8) (2010) 2040–2050, doi:10.1016/j.jas.2010.03.009.
[7] H. Mytum, J.R. Peterson, The application of reflectance transformation imaging (RTI) in historical archaeology, Hist. Archaeol. 52 (2) (2018) 489–503, doi:10.1007/s41636-018-0107-x.
[8] P. Lech, M. Matera, P. Zakrzewski, Using Reflectance Transformation Imaging (RTI) to document ancient amphora stamps from Tanais, Russia. Reflections on first approach to their digitalisation, J. Archaeol. Sci. Reports 36 (2021), doi:10.1016/j.jasrep.2021.102839.
[9] L.W. Macdonald, "Colour and directionality in surface reflectance."

[10] R. Boute, M. Hupkes, N. Kollaard, S. Wouda, K. Seymour, L. Ten Wolde, Revisiting Reflectance Transformation Imaging (RTI): a tool for monitoring and evaluating conservation treatments, IOP Conference Series: Materials Science and Engineering, 364, 2018, doi:10.1088/1757-899X/364/1/012060.
[11] J. Min et al., "Reflectance transformation imaging for documenting changes through treatment of Joseon dynasty coins," doi: 10.1186/s40494-021-00584-3.
[12] N. Rossetti, L. Stephant, N. Guilminot, E. Aubert, J.G. Melard, "Study and conservation of lead curse tablets, in: ICOM-CC MWG, Metal, 2019, p. 2019.
[13] T. Ono, S. Matsuda, Y. Mizuochi, Development of a multispectral RTI system to evaluate varnish cleaning, ICOM-CC 18th Triennial Conference, 2017.
[14] M. Li, Z. Zhou, Z. Wu, B. Shi, C. Diao, P. Tan, Multi-view photometric stereo: a robust solution and benchmark dataset for spatially varying isotropic materials, IEEE Trans. Image Process. 29 (2020) 4159–4173, doi:10.1109/TIP.2020.2968818.
[15] R. Pintus, T. Dulecha, A. Jaspe, A. Giachetti, I. Ciortan, and E. Gobbetti, "Objective and subjective evaluation of virtual relighting from reflectance transformation imaging data," doi:10.2312/gch.20181344.
[16] M. Manfredi, et al., Measuring changes in cultural heritage objects with Reflectance Transformation Imaging, in: Proc. Digit. 2013 - Fed. 19th Int'l VSMM, 10th Eurographics GCH, 2nd UNESCO Mem. World Conf. Plus Spec. Sess. fromCAA, Arqueol. 2.0 al, 1, 2013, pp. 189–192, doi:10.1109/DigitalHeritage.2013.6743730.
[17] M. Manfredi, et al., A new quantitative method for the non-invasive documentation of morphological damage in paintings using RTI surface normals, Sensors (Switzerland) 14 (7) (Jul. 2014) 12271–12284, doi:10.3390/s140712271.
[18] T.G. Dulecha, A. Giachetti, R. Pintus, I. Ciortan, A. Jaspe, E. Gobbetti, Crack Detection in Single- and Multi-Light images of painted surfaces using convolutional neural networks, GCH 2019 - Eurographics Work. Graph. Cult. Herit. (2019) 43–50, doi:10.2312/gch.20191347.
[19] V. Corregidor, R. Dias, N. Catarino, C. Cruz, L.C. Alves, J. Cruz, Arduino-controlled Reflectance Transformation Imaging to the study of cultural heritage objects, SN Appl. Sci. 2 (9) (Sep. 2020), doi:10.1007/S42452-020-03343-4.
[20] G. Earl, et al., Reflectance transformation imaging systems for ancient documentary artefacts, Electronic Visualisation and the Arts (EVA 2011) (EVA), 2011, doi:10.14236/ewic/EVA2011.27.
[21] C.H. Imaging, "Highlight – Reflectance Transformation Imaging (H-RTI) for heritage applications," no. April, pp. 1–18, 2016.
[22] H. England, "Multi-light Imaging. Highlight-Reflectance Transformation Imaging (H-RTI) for cultural heritage," 2018.
[23] R. Luxman, et al., LightBot: a multi-light robotic acquisition system for adaptive capturing of Cultural Heritage surfaces and its applicability on performing RTI data stitching, workshop on e-Heritage and Robotics, IEEE/RSJ IROS 2021, 2021.
[24] M. Zhang, M.S. Drew, Efficient robust image interpolation and surface properties using polynomial texture mapping, Eurasip J. Image Video Process. 2014 (2014) 1–19, doi:10.1186/1687-5281-2014-25.
[25] G. Pitard, G.Le Goïc, H. Favrelière, S. Samper, S.-.F. Desage, M. Pillet, Discrete Modal Decomposition for surface appearance modelling and rendering, Opt. Meas. Syst. Ind. Insp. IX 9525 (2015) 952523, doi:10.1117/12.2184840.
[26] T.G. Dulecha, ·. Filippo, A. Fanni, F. Ponchio, F. Pellacini, A. Giachetti, Neural reflectance transformation imaging, Vis. Comput. 36 (1910) 2161–2174, doi:10.1007/s00371-020-01910-9.
[27] M. Nurit, "Numérisation Et Caractérisation De L'apparence Des Surfaces Manufacturées Pour L'inspection Visuelle, Université de Bourgogne, 2022.
[28] W. Vogt, Mahalanobis distance, Dict. Stat. Methodol. (2015) 1–3, doi:10.4135/9781412983907.n1108.
[29] P. Bajorski, Statistics for Imaging, Optics, and Photonics 808 (2011).
[30] O.A. Carvalho Júnior, R.F. Guimarães, A.R. Gillespie, N.C. Silva, R.A.T. Gomes, A new approach to change vector analysis using distance and similarity measures, Remote Sens. 3 (11) (2011) 2473–2493, doi:10.3390/rs3112473.
[31] R. Wang, J.W. Chen, Y. Wang, L. Jiao, M. Wang, SAR image change detection via spatial metric learning with an improved mahalanobis distance, IEEE Geosci. Remote Sens. Lett. 17 (1) (2020) 77–81, doi:10.1109/LGRS.2019.2915251.
[32] J.W.E. Pearce, The Roman Imperial Coinage, Volume IX, Valentinian I - Theodosius I, 1933 London.